LA-8036-PR

Progress Report

C.3

Applied Nuclear Data Research and Development

April 1—June 30, 1979

LOS ALAMOS SCIENTIFIC LABORATORY
Post Office Box 1663 Los Alamos. New Mexico 87545

The four most recent reports in this series, unclassified, are LA-7482-PR, LA-7596-PR, LA-7722-PR, and LA-7843-PR.

This report was not edited by the Technical Information staff.

This work was performed under the auspices of the US Department of Energy's Office of Military Application, Division of Reactor Research and Technology, Office of Basic Energy Sciences, and Office of Fusion Energy; and the Electric Power Research Institute.

UNITED STATES
DEPARTMENT OF ENERGY
CONTRACT W-7405-ENG. 36

LA-8036-PR
Progress Report
UC-34c
Issued: September 1979

Applied Nuclear Data Research and Development

April 1—June 30, 1979

C. I. Baxman
P. G. Young

CONTENTS

APPLIED NUCLEAR DATA RESEARCH AND DEVELOPMENT
QUARTERLY PROGRESS REPORT
April 1 - June 30, 1979

Compiled by

C. I. Baxman and P. G. Young

ABSTRACT

This progress report describes the activities of the Los Alamos Nuclear Data Group for the period April 1 through June 30, 1979. The topical content is summarized in the contents.

I. THEORY AND EVALUATION OF NUCLEAR CROSS SECTIONS

A. $^{6}Li(p,^{3}He)$ Cross Section [G. M. Hale; D. C. Dodder; and S. D. Baker and E. K. Biegert (Rice University)]

The $^{6}Li(p,^{3}He)$ reaction is of interest at very low energies in connection with astrophysical questions about the relative abundances of ^{6}Li and ^{7}Li and recently has been receiving attention at higher energies as a possible exotic fuel for fusion energy applications. Reliable integrated cross sections for this reaction have been difficult to obtain in view of discrepancies as large as 50% among the measurements.

Predictions for this cross section have been available for more than two years from our multichannel R-matrix analyses of reactions in the ^{7}Be system and charge-independent analysis of reactions in the ^{7}Be and ^{7}Li systems. These results have been described in part in previous progress reports[1-4] and at the Harwell Conference.[5] Since the experimental cross-section data included in the analysis for the $^{6}Li(p,^{3}He)$ reaction required extensive renormalization in almost every case, we have been uncertain about the reliability of the scale of our calculated cross sections, which presumably was determined by data for other reactions in the analysis [e.g., $^{4}He(^{3}He,^{3}He)^{4}He$ and $^{6}Li(p,p)^{6}Li$ in the ^{7}Be analysis].

Recently, new absolute measurements of $^{6}Li(p,^{3}He)^{4}He$ angular distributions at proton energies between 0.14 and 3 MeV have been made by Elwyn et al.[6] at Argonne National Laboratory. A comparison of their integrated cross sections with our predictions is shown in Fig. 1. It can be seen that the agreement of the calculations with the new measurements is excellent, both in shape and magnitude. The agreement of the calculated angular distributions with the new data[6] is generally good at energies below 1.5 MeV; above that energy, interference effects with p-^{6}Li d-waves, which were neglected in the calculation, appear to prevent good agreement with the measured angular distribution, although they have no effect on the integrated cross sections.

This comparison indicates that the other 7-nucleon data in the analyses, through unitary and charge-conjugate relationships, correctly determined the scale of the $^{6}Li(p,^{3}He)$ reaction cross section, much as other ^{7}Li data had constrained values of the $^{6}Li(n,t)$ cross section in the analysis[7] used for the ENDF/B-V ^{6}Li evaluation at low energies. A paper[8] reporting values of the low-energy cross sections and an expression of the astrophysical s-function has been submitted to Astrophysical Journal.

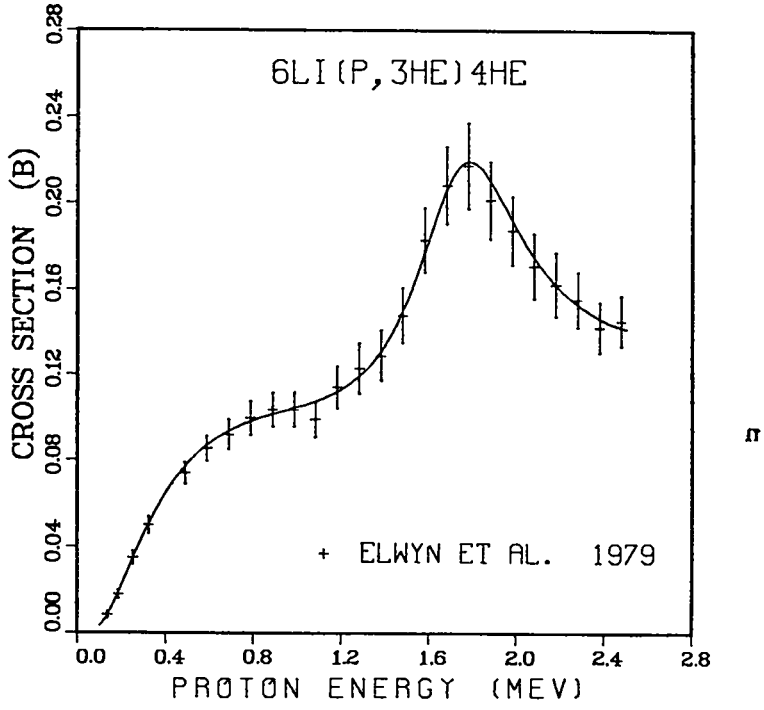

Fig. 1.
Predictions from the charge-symmetric 7-nucleon analysis[5] compared with recent measurements of Elwyn et al.[6] for the $^{6}Li(p,^{3}He)^{4}He$ integrated cross section.

B. n + ^{9}Be Evaluation (P. G. Young and L. Stewart)

A report[9] has been written describing the Los Alamos Scientific Laboratory (LASL) evaluation of n + ^{9}Be reactions, which covers the energy range 10^{-5} eV to 20 MeV. In the evaluation particular emphasis was placed on accurately representing new measurements of secondary neutron-emission spectra[10] and scattering data between 6 and 15 MeV.[11] Additionally, adjustments to the total, (n,γ), and (n,t) cross sections from previous ENDF/B evaluations were made, and covariance data files containing error correlations for cross sections and emission spectra were obtained. Detailed comparisons of experimental and evaluated data are presented in the report, and the new evaluation is found to represent the neutron emission spectra data[10] much more accurately than ENDF/B-V. The evaluated data are available in ENDF/B format from the ENDF/A library at the National Nuclear Data Center at Brookhaven National Laboratory and from the Radiation Shielding Information Center at Oak Ridge National Laboratory.

C. Arsenic Calculations (E. D. Arthur)

Calculations of neutron-induced reactions on ^{74,75}As isotopes have been made in the energy range between 0.001 and 20 MeV. The reactions for which cross sections were calculated, their Q values and thresholds are given in Table I. For this effort, a similar approach to that used for our n + Y calculations[12] was followed. That is, independent data [neutron total cross sections, resonance parameters, and (p,n) results] were used in a determination of consistent sets of neutron and proton optical model parameters. For example, Fig. 2 compares our calculated total cross section to experimental data for n + ^{75}As. The neutron optical parameters appear in Table II.

For ^{75}As, the (n,np) threshold is about 3.5 MeV lower than that for the (n,2n) reaction. This leads to an incident energy region in which the total proton production cross section can be sensitive to the parameters used to describe low energy proton emission. Therefore, we used a proton optical parameter set similar to that from our n + Y calculations and adjusted it slightly to produce agreement with low-energy (p,n) measurements. In Fig. 3, ^{74}Ge(p,n) cross sections calculated with these parameters and the neutron parameters of Table III are compared to experimental data of Johnson et al.[13] Along with both neutron and proton parameter determinations, the gamma-ray strength function was obtained through fits to ^{75}As capture data.

TABLE I

Q VALUES AND THRESHOLDS FOR n + As REACTIONS

	MT	Reaction	Q (MeV)	E_{th} (MeV)
^{74}As	4	$^{74}As(n,n')^{74}As$	-0.173	0.175
	16	$^{74}As(n,2n)^{73}As$	-7.977	8.086
	16	$^{74}As(n,2n)^{73m}As$	-8.475	8.59
	22	$^{74}As(n,n\alpha)^{70}Ga$	-4.378	4.437
	28	$^{74}As(n,np)^{73}Ge$	-6.854	6.948
	102	$^{74}As(n,\gamma)^{75}As$	10.243	0.
	102	$^{74}As(n,\gamma)^{75m}As$	9.939	0.
	103	$^{74}As(n,p)^{74}Ge$	3.346	0.
	107	$^{74}As(n,\alpha + n,\alpha n)^{70,71}Ga$	4.926	0.
^{75}As	4	$^{75}As(n,n')^{75}As$	-0.198	0.201
	16	$^{75}As(n,2n)^{74}As$	-10.243	10.38
	17	$^{75}As(n,3n)^{73}As$	-18.22	18.465
	22	$^{75}As(n,n\alpha)^{71}Ga$	-5.316	5.39
	28	$^{75}As(n,np)^{74}Ge$	-6.896	6.989
	54	$^{75}As(n,n')^{75m}As$	-0.304	0.308
	102	$^{75}As(n,\gamma)^{76}As$	7.33	0.
	103	$^{75}As(n,p)^{75}Ge$	-0.407	0.413
	103	$^{75}As(n,p)^{75m}Ge$	-0.547	0.554
	107	$^{75}As(n,\alpha + n,\alpha n)^{71,72}Ga$	1.205	0.

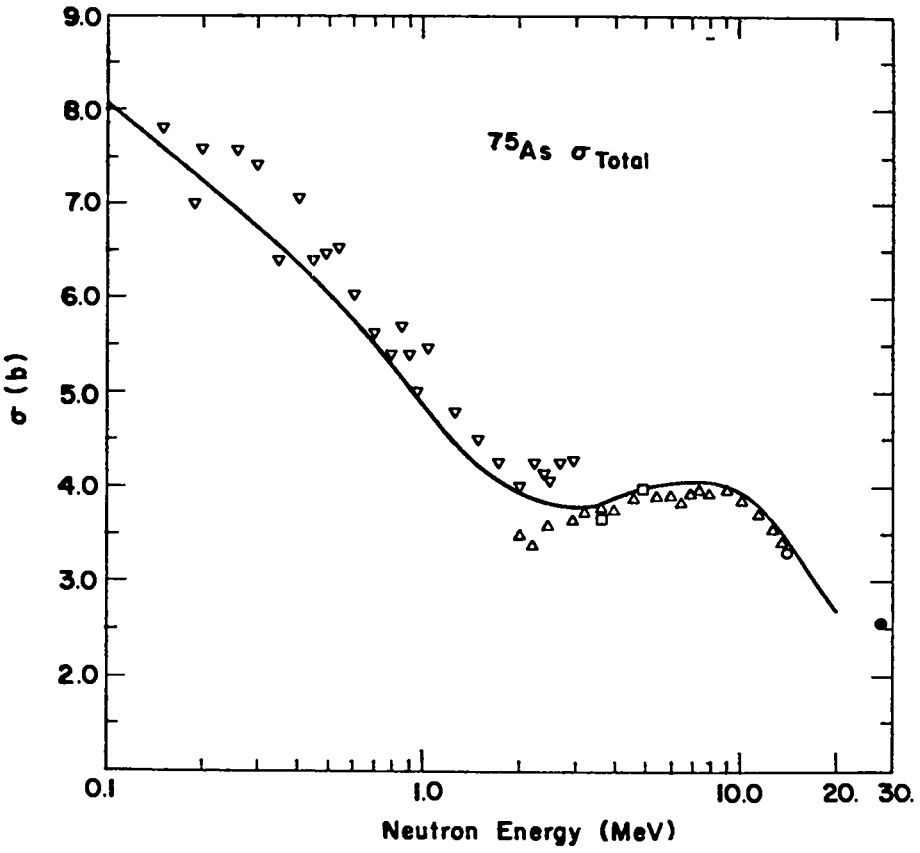

Fig. 2.
Fit to the ^{75}As total cross section using the parameters of Table II.

TABLE II

n + ^{75}As NEUTRON OPTICAL PARAMETERS

Strength (MeV)	r (fm)	a (fm)
V = 49.96 - 0.4E	1.236	0.6
W (Saxon Derivative) = 7.8 - 0.11E	1.26	0.69
V_{SO} = 6.2	1.12	0.47

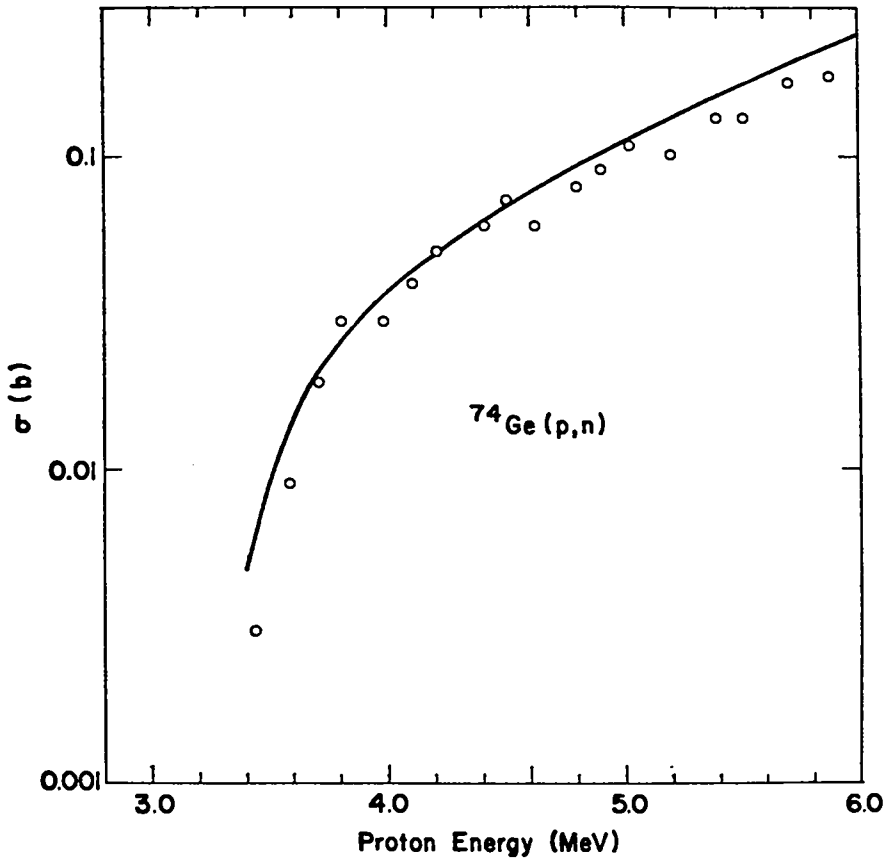

Fig. 3.
The ^{74}Ge(p,n) cross section calculated with the proton optical parameters of Table III is compared to the results of Johnson.[13]

TABLE III

PROTON OPTICAL PARAMETERS USED IN n + As CALCULATIONS

Strength (MeV)	r (fm)	a (fm)
V = 63.8 - 0.32E	1.225	0.665
W (Saxon Derivative) 3.0 + 0.6E	1.225	0.4
V_{SO} = 6.4	1.03	0.63

These parameters were used in the COMNUC and GNASH statistical model codes along with discrete level information, the Gilbert-Cameron level density model, and preequilibrium corrections made using the Kalbach exciton model. Good agreement was obtained in comparisons of our calculated results to experimental data without need for further parameter adjustments. As an example, our calculated values for the ^{75}As(n,2n) reaction are compared with experimental data in Fig. 4. Also shown by the dashed line is the calculated ^{74}As(n,2n) cross section.

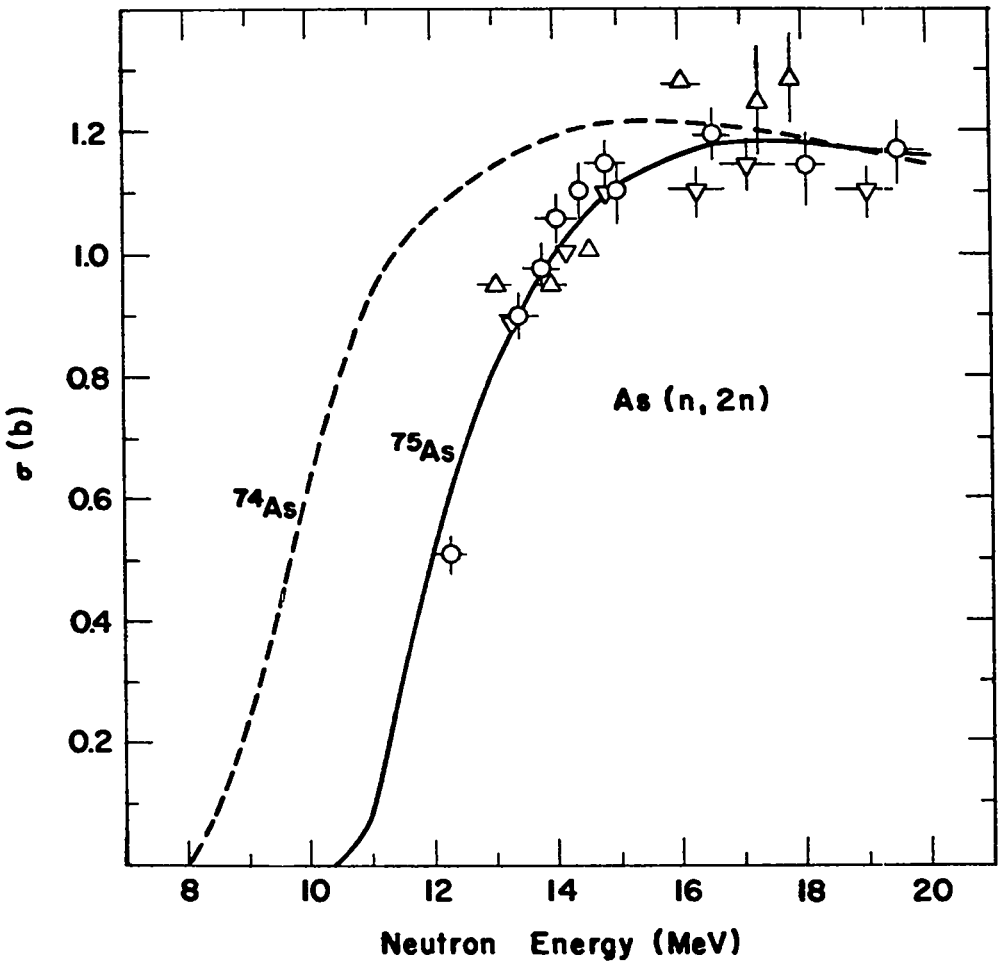

Fig. 4.
Calculated and experimental ^{75}As(n,2n) cross sections. In addition, the ^{74}As(n,2n) cross section is shown by the dashed curve.

D. Erratum: Calculation of Neutron-Induced Cross Sections on Isotopes of Iridium (E. D. Arthur)

On page 9 of LA-7843-PR, the threshold for the $^{193}Ir(n,3n)$ reaction was incorrectly listed as 14.64 MeV, while for the $^{193}Ir(n,n')^{193m}Ir$ reaction, the Q value and threshold energy were listed as -0.803 and 0.807 MeV. The correct values for these quantities are

Reaction	Q (MeV)	E_{th} (MeV)
$^{193}Ir(n,3n)^{191}Ir$	-13.97	14.04
$^{193}Ir(n,n')^{193m}Ir$	-0.0803	0.0807

Neither the results of the calculations nor the file of evaluated cross sections are influenced by these errors.

E. Average Neutronic Properties of "Prompt" Fission Products (E. D. Arthur and D. G. Foster, Jr.)

The neutronic properties of mixtures of fission products before the first beta decay takes place would be very useful to know with moderate accuracy for a number of applications. We are preparing cross sections that should represent a reasonable average for fission products from fast-neutron-induced fission of ^{235}U and ^{239}Pu. Since most of the roughly 1000 nuclides involved are far from the line of beta stability, clearly we must rely almost entirely on average properties deduced from nuclear models, except for simple properties of the ground and first few excited states.

We have chosen a weighted average over a few selected nuclides as a crude approximation to the sum over all nuclides. These nuclides are chosen from the maximum and the half-value points of the yield curves for both low- and high-mass fragments, using distinct sets for ^{235}U and ^{239}Pu fission. The resulting 19 nuclides are listed in Table IV. For each of these as a target, we are calculating cross sections for the (n,γ), (n,n'), (n,2n), and (n,3n) reactions, together with their neutron spectra and angular distributions, for incident-neutron energies from 10^{-3} to 20 MeV.

Approximately half of the 44 nuclides involved in these reactions with the specified targets lie outside the range for which mass excesses have been measured, but there are at least a few excited states reasonably well determined for most of the required nuclei. We are using adjusted masses given in the 1977 Nuclear Wallet Cards (including some "taken from nuclear systematics"), supplemented

by extrapolations using the Garvey-Kelson relations. We have used simple shell-model arguments* to identify the levels in level schemes that are otherwise largely complete and to supply a few missing ground-state spins or parities.

In addition to discrete levels, level density information, neutron optical parameters, and gamma-ray strength functions are employed in the model calculations described here. To represent the continuum excitation energy region where no discrete level information exists, we are using the Gilbert-Cameron level-density expressions with the Cook parameters, as obtained from a systematic study of resonance spacings near the neutron binding energy.

To determine neutron optical-model parameters, we rely on total cross sections along with resonance data (s- and p-wave strengths) for stable isotopes of the elements shown in Table IV. The variation of the resonance data as a function of the quantity (N-Z)/A for a particular Z permits our determining the isospin dependence of both the real and imaginary portions of the neutron optical potential. As an example, the calculated total cross section using the parameters of Table V for n + Xe is compared to experimental data in Fig. 5. In Fig. 6, calculated s-wave strengths for isotopes of xenon having A = 128-138 are compared to experimental results.

To describe gamma-ray emission both in the calculation of capture cross sections and in competition with (n,2n) and (n,3n) reactions, we have chosen the Brink-Axel giant dipole resonance (GDR) form for gamma-ray transmission coefficients. Instead of normalizing these transmission coefficients to the ratio $\frac{2\pi\langle\Gamma_\gamma\rangle}{\langle D\rangle}$, where $\langle\Gamma_\gamma\rangle$ and $\langle D\rangle$ are the average gamma-ray width and spacing for s-wave resonances, we have determined gamma-ray strength functions from fits to stable-isotope capture cross sections. Otherwise, since most of the nuclei of interest here have no information pertaining to $\langle\Gamma_\gamma\rangle$ and $\langle D\rangle$ we would have to estimate their values based on the systematic behavior of these quantities. This could lead to considerable uncertainty in the determination of $\frac{2\pi\langle\Gamma_\gamma\rangle}{\langle D\rangle}$ which would directly influence gamma-ray emission cross sections. The use of gamma-ray strength functions should alleviate many of these problems since their behavior is expected to vary slowly from isotope to isotope, thereby producing more reliable results when extrapolated to unstable nuclei.

---

*We are grateful to D. G. Madland for these estimates.

TABLE IV

NUCLIDES USED FOR FISSION PRODUCT CALCULATIONS

	^{235}U	^{239}Pu
Lower Peak		
Low	$^{87,88}Se$	$^{92,93}Kr$
Center	$^{94,95}Sr$	$^{99,100}Zr$
High	$^{102,103}Zr$	$^{107,108}Mo$
Higher Peak		
Low	^{131}Sn	^{130}Sn
Center	$^{138,139}Xe$	$^{137,138}Xe$
High	^{146}Ba	^{145}Ba

TABLE V

NEUTRON OPTICAL PARAMETERS USED FOR
n + Xe CALCULATIONS

Strength (MeV)	r (fm)	a (fm)
$V = 55.4 - 50\eta - 0.35E$	1.25	0.65
W (Saxon Deriv.) = $12.8 - 50\eta + 0.4E$	1.25	0.56
W (maximum) $= 17.1 - 50\eta$		
$V_{SO} = 7.5$	1.25	0.65

$\eta = (N-Z)/A$

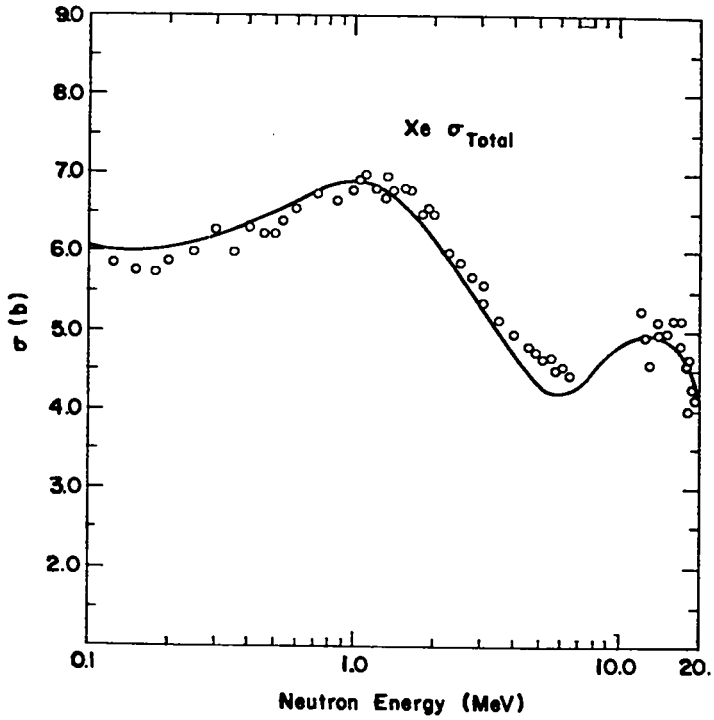

Fig. 5.
Comparison of calculated and experimental values for n + Xe.

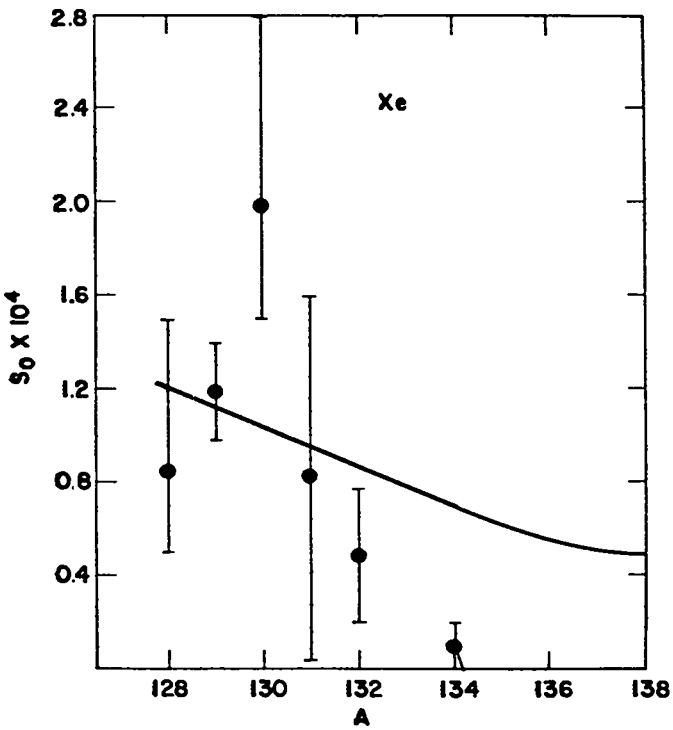

Fig. 6.
Calculated and experimental dependence of the s-wave strength, S_0, on (N-Z)/A for isotopes of xenon.

We are using COMNUC and GNASH for the actual calculations of cross sections and spectra. Neither code can cover the entire energy range of interest with acceptable accuracy. COMNUC includes width-fluctuation corrections that are important at low excitation energies and calculates angular distributions within the Hauser-Feshbach approximation, but it does not treat preequilibrium processes nor calculate neutron spectra. Thus, it is most useful for low incident energies. GNASH calculates spectra but not angular distributions, lacks width-fluctuation corrections but includes preequilibrium effects, so that it is most useful at higher energies, especially above the (n,2n) and (n,3n) thresholds. We intend to use a simple optical model to supply the angular distribution from elastic scattering that is absent from the GNASH calculations. We have modified GNASH to write disk files of the constituents of the neutron spectra, so that these can be summed for the files expected in ENDF/B.

At the end of the quarter, all input data had been collected, and all COMNUC calculations had been carried out and stored. Modifications to GNASH are almost complete. We expect the GNASH calculations and collection of the results into a single average ENDF/B file to require another quarter's work.

F. GNASH Improvements (E. D. Arthur)

The GNASH preequilibrium-statistical model code has been modified so that the amount of central processor time (CPU) used is about half that of previous versions. The change involved elimination of two computational loops in which the total and partial widths, Γ_{tot} and Γ_i, were calculated separately. Now the partial widths are normalized concurrently by the total width for each compound nucleus spin and parity state, resulting in only one pass through the loop. The total running times (I/O and CPU) between the present and older GNASH versions are compared in Table VI.

In addition, several other changes have been made. The ability to produce population information so that complex spectra can be obtained has been reinstated along with the ability to provide for the existence of target nuclei in excited states. The representation of the gamma-ray strength function has been improved to include a two-Lorentz line description of the giant dipole resonance (GDR), a step in the GDR tail, and the possibility of a pygmy resonance occurring at energies lower than the GDR.

G. CSEWG Activities (G. M. Hale, L. Stewart, and P. G. Young)

1. Dosimetry Special Purpose Files. Files for the ^{6}Li and ^{10}B total helium production cross sections and the $^{27}Al(n,p)$ and (n,α) cross sections were prepared and sent to the National Nuclear Data Center for incorporation into the Version V Special Dosimetry File. Error files (File 33 data) are included for each of the cross sections listed above.

2. Standard Reference and Other Important Nuclear Data. A status report on this subject is being prepared by the CSEWG Normalization and Standards Subcommittee. Papers on H(n,n) scattering,[14] the $^{6}Li(n,\alpha)$ and $^{10}B(n,\alpha)$ reactions, and prompt fission neutron spectra have been prepared at LASL for inclusion in this report. Contributions from other laboratories have been critically reviewed as requested.

TABLE VI

GNASH RUNNING TIME COMPARISONS (CDC 7600)

Problem	Total 7600 Time (I/O + CPU) Old Version	New Version
^{184}W, E_n = 12 MeV, ΔE = 1.0 MeV	20.1 s	9.93 s
^{184}W, E_n = 20 MeV, ΔE = 1.0 MeV	47	27.7
^{184}W, E_n = 14 MeV, ΔE = 0.5 MeV	36.2	23

II. NUCLEAR CROSS SECTION PROCESSING

A. Cross Section Production (R. B. Kidman, R. M. Boicourt, and R. E. MacFarlane)

The ENDF/B-V general purpose files have been released (139 nuclides), and they are now being processed using NJOY. So far, 75 nuclides have been processed into pointwise form (PENDF), 61 nuclides have been converted to multigroup constants (30 neutron groups and 12 photon groups at 300 K and infinite dilution), and 28 nuclides are available for continuous-energy Monte-Carlo calculations. During the next quarter, additional materials and group structures will be formatted into libraries to be used for testing ENDF/B-V.

B. Energy Balance of ENDF/B-V (R. E. MacFarlane)

The latest version of the Evaluated Nuclear Data Files (ENDF/B-V)[15] contains photon production data for 24 fissionable and 36 nonfissionable materials. It therefore provides a nearly comprehensive source of data for coupled neutron-photon transport calculations of heat deposition and radiation exposure. Before these data may be used with confidence, they must be tested. In the standard ENDF testing procedure, the files are used to compute the photon production for a set of benchmarks. Unfortunately, the state of the art is such that 10 to 20% agreement is considered very good.[16] Furthermore, many materials are not tested by the existing experimental benchmarks. As introduced in previous reports,[17,18] the traditional tests can be supplemented with an energy balance analysis that finally results in a rating of the usefulness of each ENDF/B-V material for exacting heat/dose calculations.

The kinetic energy released in a material (KERMA) due to a neutron reaction is just the energy available (E+Q) less the energy carried away by secondary neutrons and photons.[19] This secondary energy is transported elsewhere in the coupled calculation and deposited in subsequent reactions. Clearly, in a system large with respect to neutron and photon mean-free paths, the heating depends only on flux, cross section, and Q-value; it is independent of the details of neutron and photon spectra and yields.

This KERMA factor is a sensitive test of the energy balance of an evaluation. As an example, if the evaluation gives too much energy to secondary photons, the KERMA can be negative. In a large system, this negative number would exactly cancel the excess heating due to the hot photons, but in a small system, the photons might escape. The calculation would predict a net cooling effect.

Meanwhile, the photons would cause an overestimate of the heating or radiation dose elsewhere. Equally serious problems arise if the energy-balance KERMA factor is too large.

In many cases, reasonable bounds may be placed upon the KERMA factors by kinematics. The average recoil energy can be computed accurately for two-body scattering (elastic or inelastic) and radiative capture. For a reaction like (n,α), bounds can be established by taking the limit where all available energy comes out with the alpha or the limit where the alpha is emitted with zero energy. Similar arguments can be used for other reactions. The HEATR module of the NJOY cross-section processing system[20] has been coded to compare the energy-balance KERMA factors with their kinematic limits and to produce informative diagnostics whenever the limits are violated.

For the natural element evaluations, the kinematic checks are less useful since the isotopic cross sections and Q-values needed to compute the available energy are not included in the ENDF/B format. However, useful indications are still obtained for energy regions dominated by elastic or inelastic scattering.

These energy-balance checks have been carried out for most of the nonfissionable materials from ENDF/B-V with photon production data. The results are summarized qualitatively in Table VII for three different energy ranges: THER (below 1 keV), FAST (1 keV-2 MeV), FUSN (2-20 MeV). The usefulness of the data in each range is classified as G (good), F (fair, possibly adequate for minor materials or mid-size regions), or P (poor, adequate only for trace elements or large systems).

An inspection of the table shows that the light isotopes are in good shape; that stainless steels should be treated with caution, especially at high energies; and that copper and the heavy metals may give poor answers when used in small pieces (e.g., coils for magnetic fusion machines).

Efforts are underway in the ENDF community to resolve the more important discrepancies (e.g., the tungsten isotopes are being reevaluated at Los Alamos and iron KERMA factors are being calculated for the Fusion Materials Irradiation Test Facility at Hanford). This study suggests that evaluators should (1) do isotopic evaluations when possible, (2) use model codes wherever practical, (3) avoid placing experimental data directly into the files without analysis, (4) use yields rather than production cross sections where possible, (5) use discrete photons rather than continuous distributions where possible, and (6) check the energy balance at each stage in the evaluation.

TABLE VII

QUALITATIVE RATING OF ENERGY BALANCE FOR MATERIALS FROM ENDF/B-V
(G=Good, F=Fair, P=Poor) BY ENERGY RANGE
(THER=<1 keV, FAST=1 keV to 2 MeV, FUSN= 2 to 20 MeV)

Material	THER	FAST	FUSN	Material	THER	FAST	FUSN
H-1	G	G	G	K	a	a	P
H-2	G	G	G	Ca	G	G	G
Li-6	G	G	G	Ti	G	F	F
Li-7	G	G	G	V	G	G	F
Be-9	G	G	G	Cr	a	a	P
B-10	G	G	G	Mn-55	P	P	P
C	G	G	G	Fe	a	F	P
N-14	G	G	G	Co-59	G	P	P
N-15	G	G	F	Ni	G	P	F
O-16	G	G	G	Cu	a	a	a
				Nb-93	P	P	F
F-19	G	G	F	Mo	a	a	a
Na-23	G	G	F	Ba-138	F[b]	F	F
Mg	G	F	F	Ta-181	P[b]	P	P
Al-27	G	G	F	W-182	G	P	P
Si	G	G	F	W-183	G	P	P
P-31	G	G	F	W-184	G	P	P
S-32	G	G	F	W-186	G	P	P
Cl	a	G	a	Pb	a	G	F

[a] Tests masked by element effect

[b] Possibly masked by internal conversion

C. An Epithermal Disadvantage Factor for EPRI-CELL (R. E. MacFarlane)

The thermal reactor fuel cycle code EPRI-CELL uses the B_1 approximation in a homogenized cell to compute the neutron absorption between 1.855 eV and 10 MeV. This calculation requires cell-averaged cross sectons rather than the zone-averaged cross sections normally produced by NJOY. Since CELL already uses cell-averaged densities, it is convenient to define a "disadvantage factor" for a cross section in zone i using flux and volume weighting,

$$D_{ig} = \frac{\sum_j V_j \phi_{ig}}{\sum_j V_j \phi_{jg}} \quad , \tag{1}$$

where the V_i and ϕ_{ig} are volumes and group fluxes for zones (zones are regions of constant cross sections, such as fuel f or moderator m). The EPRI-CELL code assumes that $\phi_m \simeq \phi_f$, so the disadvantage factors are unity.

A more realistic estimate for ϕ_f and ϕ_m can be obtained by using the standard two-region equivalence theory and assuming that all resonances are narrow with respect to moderator scattering. We obtain

$$\phi_m \sim (1-\beta)\frac{1}{E} + \beta\phi_f \quad , \tag{2}$$

where

$$\beta = \frac{V_f \Sigma_e}{V_m \Sigma_m} \quad . \tag{3}$$

Using the intermediate-resonance approximation for fuel scattering gives

$$\phi_f \sim \frac{\lambda\Sigma_p + \Sigma_e}{\Sigma_a + \lambda\Sigma_p + \Sigma_e}\ \frac{1}{E} \quad . \tag{4}$$

In these equations, Σ_e is the equivalent escape cross section, $\lambda\Sigma_p$ is the effective fuel potential scattering, Σ_m is the moderator cross section, and Σ_a is the fuel absorption cross section. Going over to multigroup notation, the two-region disadvantage factors become

$$D_{fg} = \frac{1}{1 + d\Sigma_{ag}} \quad , \tag{5}$$

and

$$D_{mg} = \frac{1 + \frac{V_m + V_f}{V_m} d\Sigma_{ag}}{1 + d\Sigma_{ag}} \quad , \tag{6}$$

where

$$d = \frac{(1-\beta)V_m}{V_f + V_m} \frac{1}{\lambda\Sigma_p + \Sigma_e} \quad . \tag{7}$$

The qualitative effect is clear from Eq. (5); the effective fuel cross section is reduced for groups with high absorption. Note that D goes to 1 for the homogeneous case (β=1).

Coding has been added to the GAM100 subroutine of EPRI-CELL to apply these factors and tested on the BAPL-UO_2-1 benchmark.[21] The results are compared with experiment, continuous energy Monte-Carlo, and the original CELL method in Table VIII. The new factor removes a large part of the discrepancy; the remainder is probably due to intermediate-resonance effects on spatial self-shielding and resonance interference.

TABLE VIII

EFFECT OF EPRI-THERMAL DISADVANTAGE FACTOR ON EPRI-CELL RESULTS FOR THE BAPL-UO_2-1 BENCHMARK (d = 0.335)

Integral Parameter	CELL W/Disad.	CELL W/o Disad.	Monte-Carlo[a]	Experiment
0.625-5530 eV U-238 group abs. cross section	2.069	2.246	2.019	
k_∞	1.1223	1.1020	1.1353	
k_{eff}	0.9877	0.9701		1.
ρ_{28}			1.383	1.39±0.01

[a] Infinite lattice calculation.

III. FISSION PRODUCTS AND ACTINIDES: YIELDS, YIELD THEORY, DECAY DATA, DEPLETION, AND BUILDUP

A. Fission Yield Theory [R. E. Pepping (University of Wisconsin); D. G. Madland; C. W. Maynard (University of Wisconsin); T. R. England; and P. G. Young]

The investigation of the fission process through the statistical model has been completed, and a detailed report of the findings is forthcoming. In it a model is developed to understand fission-product yields based upon a thermal equilibrium assumption and employing a recent nuclear mass formula and nuclear density of states formalism. An indication of the source of mass asymmetry in fission is given. Semi-quantitative agreement is obtained with measured mass-chain yields for $^{233}U(n_{th},f)$, $^{235}U(n_{th},f)$, $^{239}Pu(n_{th},f)$, $^{235}U(n_{14},f)$, $^{238}U(n_{14},f)$, and $^{252}Cf(sf)$. The validity of models currently used in the generation of data libraries is investigated. A general procedure for the estimation of fission-product yields for an arbitrary fissioning system is presented.

B. ENDF/B-V Fission Product Yields and Testing [T. R. England; D. G. Madland; B. F. Rider (General Electric); R. E. Schenter (Hanford Engineering Development Laboratory); and J. R. Liaw (Argonne National Laboratory)]

The report on ENDF/B-V yield testing is still being prepared; the supporting work is complete.

The literature has been reexamined by one of us (BFR) and verified for ∿18 000 yields and quoted errors. All of the UK experimental yields have been checked for differences with ENDF/B-V, and errors have been corrected. Questionable yields and several duplications due to the same experimental data appearing in more than one publication have been removed. Recent experimental data provided by B. Maeck and B. Wehring have been incorporated. The next mod of ENDF will incorporate the effects of these changes.

In addition, independent and cumulative yields will be added for ^{234}U, ^{238}Pu, ^{241}AM, ^{243}Am, ^{238}Np, and ^{242}Cm fast fission and for ^{240}Pu, ^{234}U, ^{236}U 14-MeV fission. We estimate these will be added within ∿ one year.

The new ENDF/B-V yields have been incorporated into the CINDER-10 library and compared with the LASL decay-heat experiment for ^{235}U and ^{239}Pu. The new yields do not significantly effect the integral decay-heat comparisons. The calculational difference with ^{239}Pu apparently resides with decay energies, not yields. Comparisons with experiment are provided in Tables IX and X.

TABLE IX

COMPARISON YARNELL AND BENDT DECAY HEAT EXPERIMENT (LA-NUREG-6713) FOR ^{235}U USING ENDF/B-IV AND V YIELDS WITH IV DECAY DATA

Cooling Time(s)	Exp MeV/F	Exp Uncertainty (1σ in %)	Calculation Using ENDF/B-IV Data	Calculation Using ENDF/B-V Yields (-IV Data)	Ratio V/IV Cal	Ratio Exp/Cal -IV	Ratio Exp/Cal -V
10	8.10	4.1	7.780	7.783	1.000	1.041	1.041
15	7.38	3.0	7.239	7.248	1.000	1.019	1.018
20	6.933	2.6	6.842	6.854	0.998	1.013	1.012
30	6.335	2.3	6.276	6.290	0.998	1.009	1.007
40	5.920	2.1	5.873	5.888	0.997	1.008	1.005
50	5.614	2.0	5.562	5.577	0.997	1.009	1.007
60	5.358	2.0	5.309	5.324	0.997	1.009	1.006
70	5.141	1.9	5.097	5.113	0.997	1.009	1.005
80	4.958	1.8	4.915	4.932	0.997	1.009	1.005
90	4.806	1.8	4.758	4.774	0.997	1.010	1.007
100	4.667	1.8	4.619	4.636	0.996	1.010	1.007
150	4.170	1.7	4.112	4.128	0.996	1.014	1.010
200	3.841	1.6	3.780	3.796	0.996	1.016	1.012
250	3.608	1.6	3.541	3.556	0.996	1.019	1.015
300	3.419	1.6	3.355	3.370	0.996	1.019	1.015
350	3.265	1.6	3.205	3.218	0.996	1.019	1.015
400	3.135	1.6	3.078	3.091	0.996	1.019	1.014
450	3.022	1.6	2.969	2.981	0.996	1.018	1.014
500	2.920	1.6	2.873	2.884	0.996	1.016	1.012
600	2.746	1.5	2.709	2.719	0.996	1.014	1.010
700	2.598	1.5	2.572	2.581	0.997	1.010	1.007
800	2.474	1.5	2.455	2.462	0.997	1.008	1.005
900	2.363	1.5	2.351	2.358	0.997	1.005	1.002
1000	2.264	1.5	2.258	2.264	0.997	1.003	1.000
1500	1.886	1.5	1.901	1.905	0.998	0.992	0.990
2000	1.627	1.5	1.650	1.652	0.999	0.986	0.985
5000	0.9111	1.5	0.9362	0.9338	1.003	0.973	0.976
8000	0.6480	1.6	0.6553	0.6521	1.005	0.989	0.994
10000	0.5401	1.7	0.5440	0.5408	1.006	0.993	0.999
15000	0.3803	1.8	0.3778	0.3751	1.007	1.007	1.014
20000	0.2918	2.0	0.2874	0.2853	1.007	1.015	1.023
30000	0.1947	2.3	0.1923	0.1910	1.007	1.012	1.019
100000	0.0454	2.2	0.0455	0.0450	1.011	0.971	1.009

TABLE X

COMPARISON YARNELL AND BENDT DECAY HEAT EXPERIMENT [NUREG/CR-0349 (LA-7452-MS)] FOR ^{239}Pu FISSION USING ENDF/B-IV AND V YIELDS WITH IV DECAY DATA

Cooling Time(s)	Exp MeV/F	Exp Uncertainty (1σ in %)	ENDF/B-IV Data	Calculation Using ENDF/B-V Yields (-IV Data)	Ratio V/IV Cal	Ratio Exp/Cal -IV	Ratio Exp/Cal -V
20	6.482	5.0	5.850	5.881	1.005	1.108	1.102
30	6.014	3.0	5.416	5.441	1.005	1.110	1.105
40	5.640	3.0	5.098	5.118	1.004	1.106	1.102
50	5.366	3.0	4.848	4.865	1.004	1.107	1.103
60	5.116	3.0	4.641	4.656	1.003	1.102	1.099
70	4.923	3.0	4.466	4.479	1.003	1.102	1.099
80	4.756	3.0	4.314	4.326	1.003	1.102	1.099
90	4.605	3.0	4.181	4.192	1.003	1.101	1.099
100	4.488	3.0	4.064	4.074	1.002	1.104	1.102
150	4.027	3.0	3.627	3.636	1.002	1.110	1.108
200	3.739	3.0	3.339	3.346	1.002	1.120	1.117
300	3.361	3.0	2.966	2.971	1.002	1.133	1.131
400	3.096	3.0	2.720	2.724	1.001	1.138	1.137
500	2.885	3.0	2.535	2.538	1.001	1.138	1.137
600	2.710	3.0	2.385	2.389	1.002	1.136	1.134
700	2.556	3.0	2.259	2.262	1.001	1.131	1.130
800	2.432	3.0	2.149	2.153	1.002	1.132	1.130
900	2.311	3.0	2.051	2.056	1.002	1.127	1.124
1000	2.206	3.0	1.964	1.969	1.003	1.123	1.120
1500	1.802	3.0	1.625	1.634	1.006	1.109	1.103
2000	1.527	3.0	1.389	1.400	1.008	1.099	1.091
5000	0.7973	3.1	0.7445	0.7536	1.012	1.071	1.058
8000	0.5457	3.1	0.5100	0.5189	1.017	1.070	1.052
10000	0.4566	4.0	0.4220	0.4287	1.016	1.082	1.065
15000	0.3226	4.0	0.2952	0.2988	1.012	1.093	1.080
20000	0.2485	4.0	0.2282	0.2303	1.009	1.089	1.079
30000	0.1721	3.9	0.1586	0.1591	1.003	1.085	1.082
40000	0.1302	3.8	0.1206	0.1209	1.002	1.080	1.077
50000	0.1044	3.4	0.0958	0.0962	1.004	1.090	1.085
81899[a]	0.0596	3.4	0.0549	0.0566	1.031	1.086	1.053
99740[a]	0.0467	3.4	0.0435	0.0434	0.998	1.074	1.076

[a]The calculated values at 81899 and 99740 s were actually for 80297 and 100000 s, respectively.

C. The Effects of Neutron Absorption on Decay Heat (R. J. LaBauve, T. R. England, and W. B. Wilson)

Neutron absorption by fission products becomes important at high-flux levels and long cooling times. The flux level can reduce the density of directly yielded products at short irradiation times, significant for nuclides having large cross sections and large yields, and neutron absorption in stable and long-lived nuclides tends to buildup the concentration of more unstable nuclides. General equations are developed in Appendix D of Ref. 22 for both positive and negative effects of absorptions using two-nuclide chains. Pairs of coupled nuclides, rather than multiple absorptions, have been found to be a sufficient representation of the effect of absorption on total heating. The equations in Ref. 22 are used with two incident neutron-energy groups (thermal and epithermal) but can be used with any group structure.

For the purpose of exposition, simplifications can be made to the generalized equations in Ref. 22 that are appropriate for a reaction such as $^{133}Cs(n,\gamma)^{134}Cs$. For the case of constant fluxes and fission rate for an irradiation time T, the absorption correction is given by the equation

$$\Delta F(t,T,\phi) = N_2(T,\phi)\lambda_2 E e^{-\lambda_2 t} \quad , \tag{8}$$

where the correction ΔF is the decay energy to be added to the calculation without absorption; t is the cooling time; λ_2 is the decay constant of the second nuclide in the two-nuclide chain (^{134}Cs in the above example); E is the average gamma-, beta-, or total-energy per decay for nuclide 2; and $N_2(T,\phi)$ is the additional atom density of nuclide 2 resulting from radiative capture in nuclide 1.

$$N_2(T,\phi) = Y_1 A_1 S \left[\frac{1}{\beta_1\beta_2} - \frac{e^{-\beta_1 T}}{\beta_1(\beta_2-\beta_1)} + \frac{e^{-\beta_2 T}}{\beta_2(\beta_2-\beta_1)} \right], \tag{9}$$

where $\beta = \lambda + \sum_{gp} \sigma\phi = \lambda + A$.

Radiative capture in nuclide 2 must also generally be included, as indicated using β_2; the general equations must also account for neutron absorption on the decay energy rate from nuclide 1 and reduction in density of nuclide 2 due to buildup from its mass chain yield.

In the equation for $N_2(T,\phi)$, Y_1 is the fission yield for the precursor nuclide in the chain (^{133}Cs in the example), T is the irradiation time at constant power represented by a thermal flux ϕ_{th} and an epithermal flux ϕ_{epi}, and S is the fission rate. Let the thermal and epithermal cross sections in the two nuclides involved in the (n,γ) reaction be represented by σ^1_{th} and σ^1_{epi} for the first nuclide and σ^2_{th} and σ^2_{epi} for the second nuclide. Also let

$$R = \phi_{epi}/\phi_{th} \quad . \tag{10}$$

Then,

$$A_1 = (\sigma^1_{th} + R\sigma^1_{epi}) \times 10^{-24}\ \phi_{th} \quad , \tag{11}$$

$$A_2 = (\sigma^2_{th} + R\sigma^2_{epi}) \times 10^{-24}\ \phi_{th} \quad , \tag{12}$$

$$\beta_1 = A_1 + \lambda_1 \quad , \tag{13}$$

$$\beta_2 = A_2 + \lambda_2 \quad . \tag{14}$$

This correction, ΔF, for a particular two-nuclide chain can then be added to the ANS 5.1 expression

$$F(t,T) = \sum_{i=1}^{23} \frac{\alpha_i}{\lambda_i}\ e^{-\lambda_i t}(1-e^{-\lambda_i T}) \quad , \tag{15}$$

for calculating decay heat after an irradiation time T and for a cooling time t, using the fitted pulse parameters α_i and λ_i.

To demonstrate the accuracy of the approximation using only two-nuclide chains, we have made calculations for ^{235}U irradiated for 20 000 hrs with thermal neutron fluxes of 10^{13} and 10^{14} n/cm^2-3 used with effective 2200 m/s cross sections and compared results with those from CINDER-10 calculations. Fission products important for absorption effects are shown in Table XI, and those two-nuclide chains used in the approximate calculations are indicated in the table (19 in toto). Note that the chains chosen include both positive and negative effects. Comparison results are shown in Figs. 7-9 for total beta, total gamma, and total beta + gamma, respectively, for fluxes of 10^{13} and 10^{14}. Note that

TABLE XI

FISSION PRODUCTS IMPORTANT IN DETERMINATION OF NEUTRON ABSORPTION EFFECTS ON DECAY POWER

Nuclide	Precursor(s)	Nuclide	Precursor(s)
$a^{90}Y$	$a^{89}Y$, $a^{90}Sr$	$a^{148}Pm$	^{147}Nd, $a^{147}Pm$
$a^{100}Tc$	$a^{99}Tc$	$a^{148}Pm$	^{147}Nd, $a^{147}Pm$
$a^{104}Rh$	$a^{103}Rh$	^{147}Pm	^{147}Nd, ^{147}Pm
^{105}Rh	^{105}Ru		^{148}Pm, ^{148m}Pm
^{116}In	^{115}In	$a^{150}Pm$	^{147}Nd, ^{147}Pm
$a^{130}I$	$a^{129}I$, ^{130m}I		^{148}Pm, ^{148m}Pm
$a^{134}Cs$	$a^{133}Cs$		$a^{149}Pm$
$a^{135}Xe$	$a^{135}I$	^{151}Sm	^{150}Sm
$a^{136}Cs$	^{135}Xe, $a^{135}Cs$	$a^{153}Sm$	$a^{152}Sm$
$a^{140}La$	$a^{140}Ba$, $a^{139}La$	$a^{154}Eu$	$a^{153}Eu$
$a^{142}Pr$	$a^{141}Pr$	$a^{156}Eu$	$a^{155}Eu$
$a^{144}Pr$	$a^{144}Ce$, $a^{143}Pr$		
^{147}Nd	^{146}Nd		

[a] Nuclides included in two-nuclide chains in CALENDA code as of June 1979. ^{135}Xe gives the major negative effect and ^{134}Cs the major positive effect.

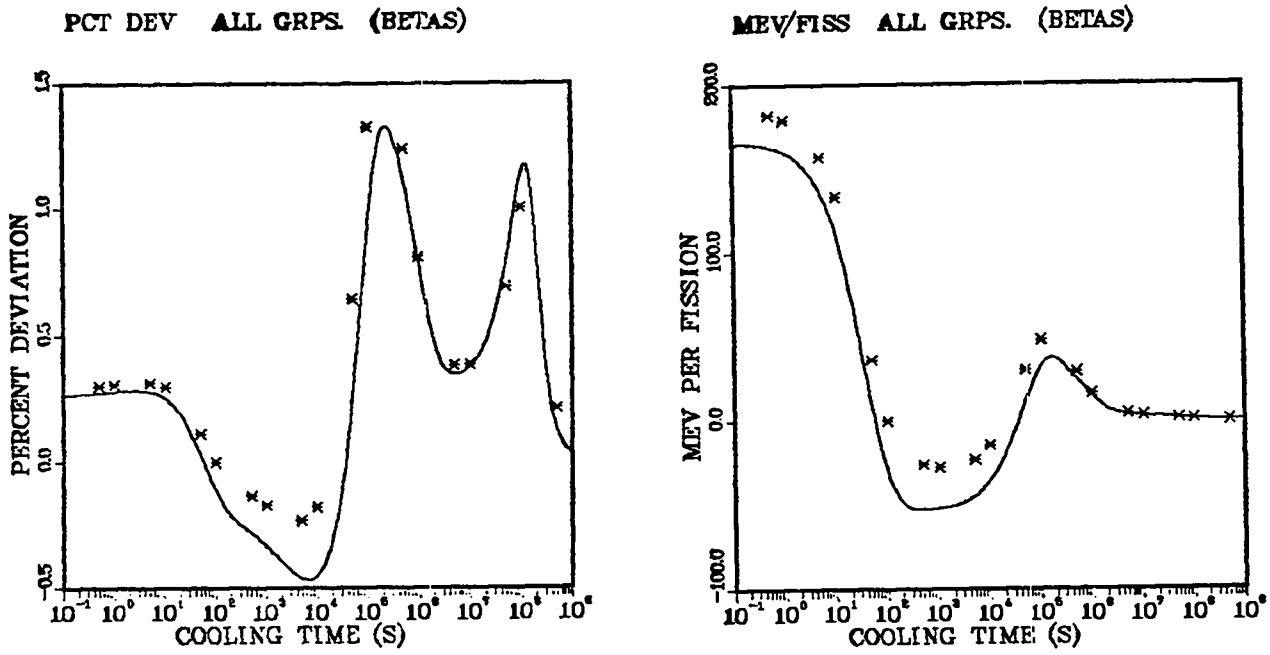

Flux = 1.E + 13

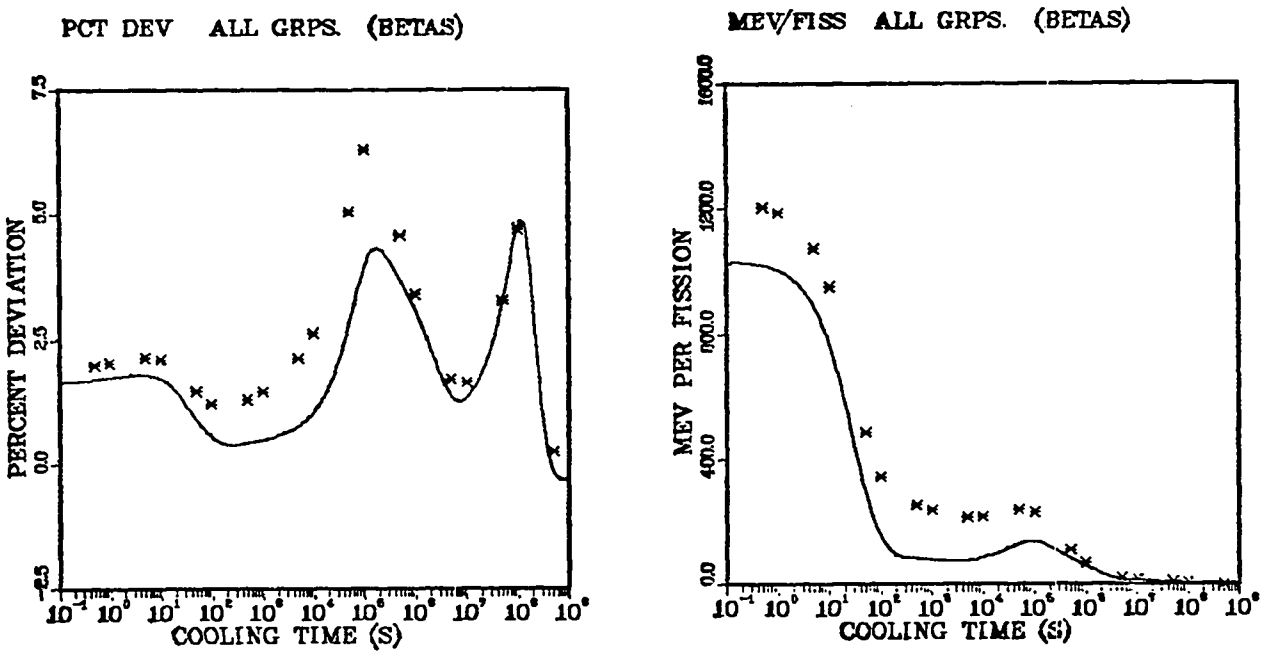

Flux = 1.E + 14

Fig. 7.
Comparison of approximate method with CINDER-10 results (betas).

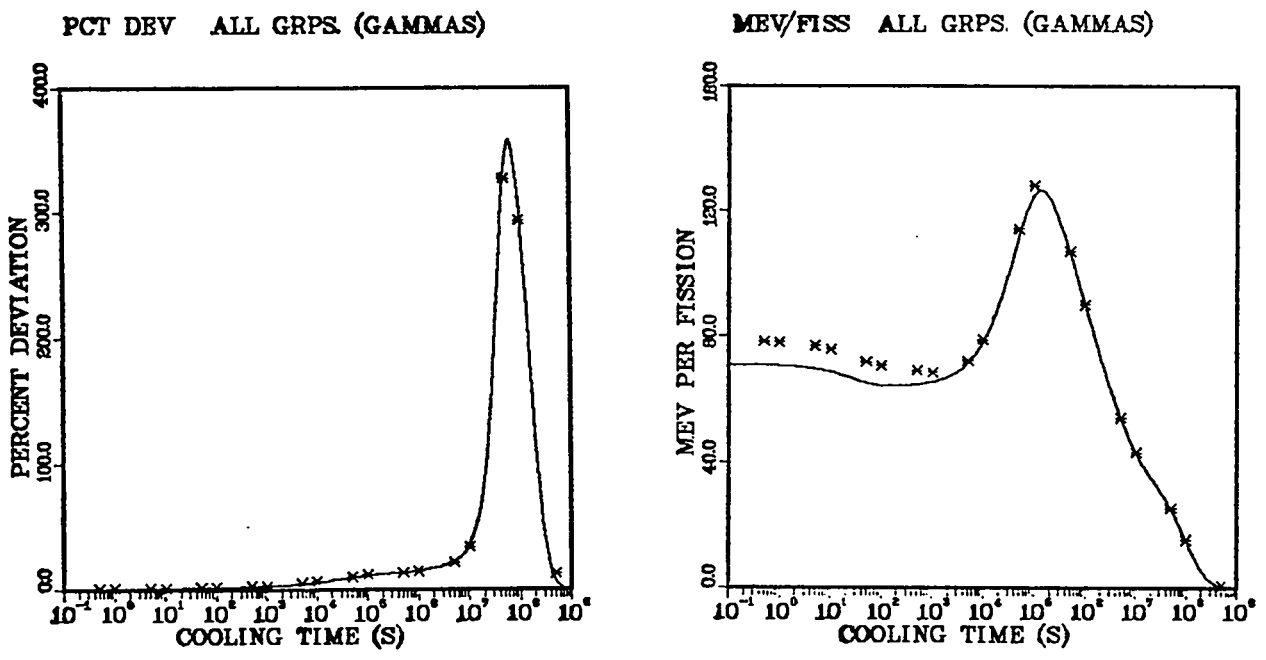

Flux = 1.E + 13

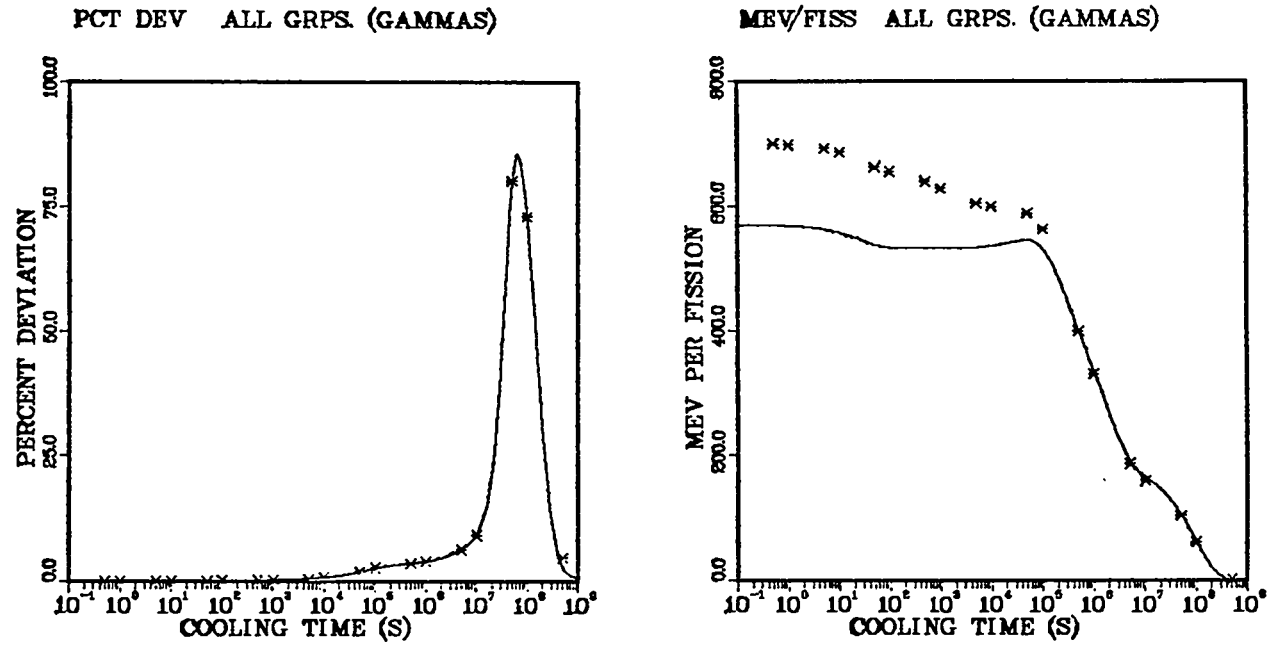

Flux = 1.E + 14

Fig. 8.
Comparison of approximate method with CINDER-10 results (gammas).

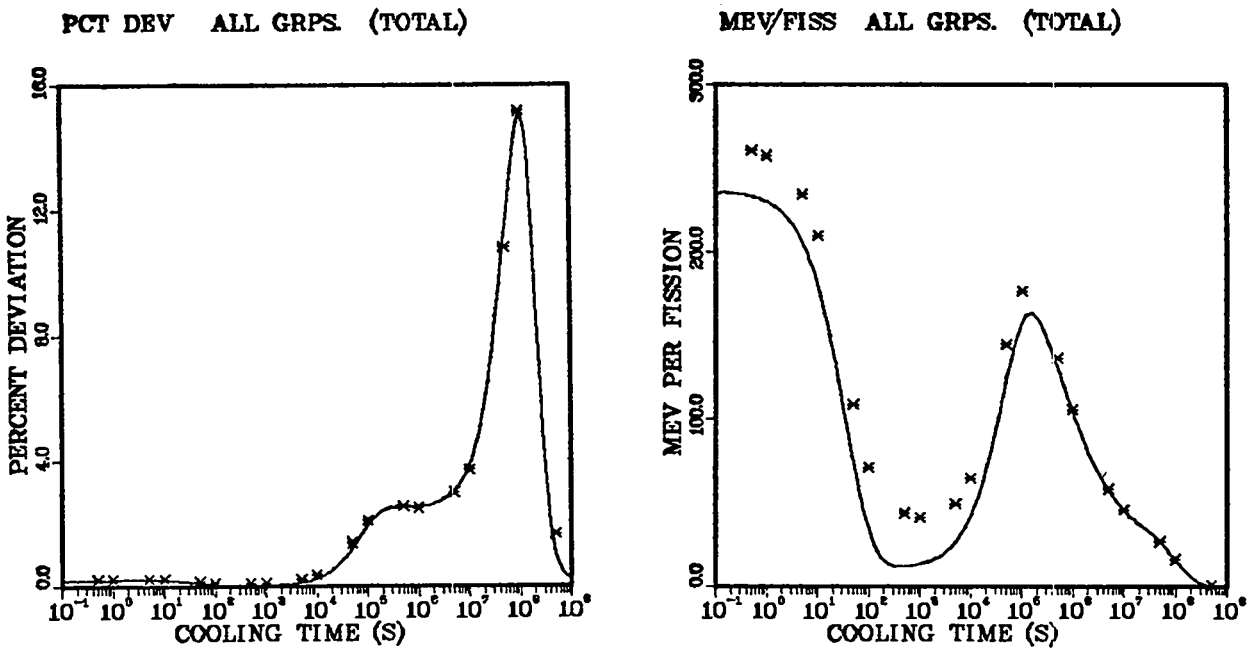

Flux = 1.E + 13

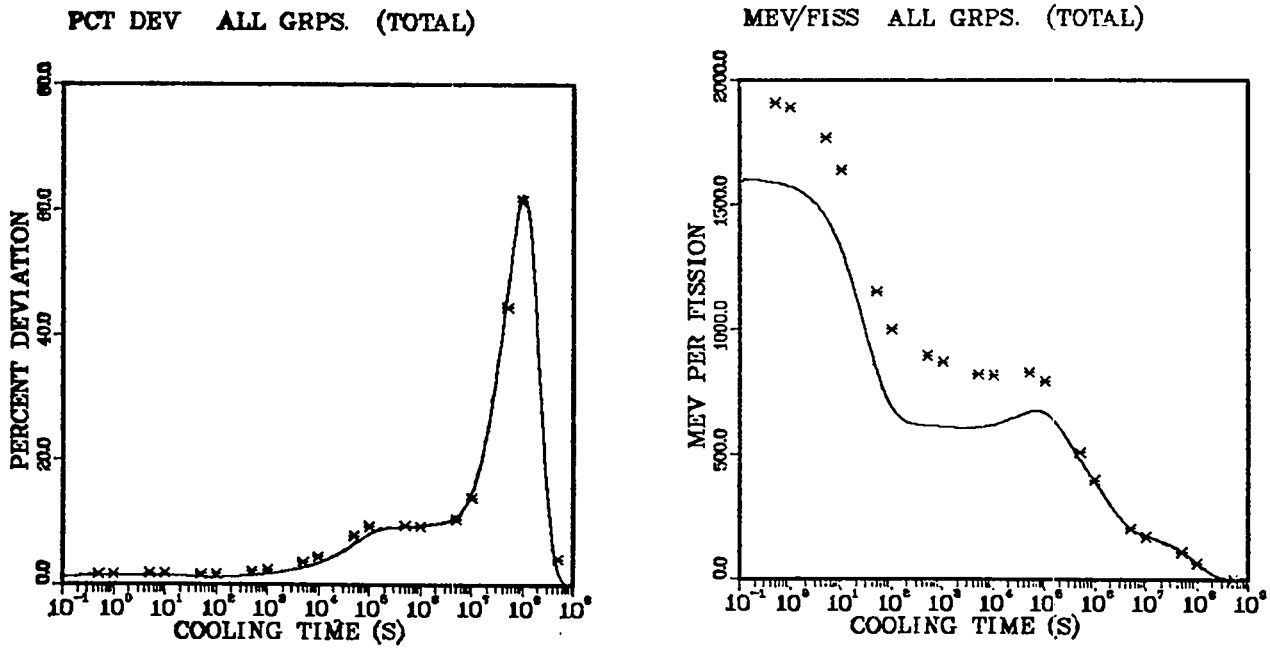

Flux = 1.E + 14

Fig. 9.
Comparison of approximate method with CINDER-10 results (total = beta + gamma).

these are expressed both as per cent deviation from the cases without absorption and as MeV/fis(x 10^4), i.e., $\sum_{i=1}^{19} F_1$. Individual points in the figures are for CINDER-10 calculations at specific cooling times; the continuous curves (actually 200 points) represent the approximate calculations. Some of the 19 chains are not very significant to total heating but are needed in a similar application to few-group spectra.[23]

As can be observed from these figures, quite accurate absorption effects can be calculated using two-nuclide chains. Moreover, the equations involved are simple and have been coded on a pocket calculator along with Eq. (15).

In order to avoid the use of approximate fits and maximum values for G(t) (the neutron absorption correction factor) in future versions of the ANS 5.1 standard, we recommend specification of an equation, as in Ref. 22, plus tabular data for its use along with a schematic or simple list of the pairs of coupled nuclides. This will require little increase in space over the current ANS 5.1 specifications. The equation is no more complicated than is currently specified for the ^{239}U and ^{239}Np actinides, and as noted in Ref. 22, it can be written in terms of a histogram representation of the power history, as is already used in the standard. We are suggesting, in effect, that the reactor and power history nature of the absorption effect can be a rather accurate model of the few actual physical nuclides affected by absorption. For LWR's, the cross sections can be provided based, e.g., on a soft spectrum, or supplied by the user based on the values already used in safety analysis reports; that is, on values justified by the user.

For fast reactors, the modeling may be simpler, and an analytic fit may even be possible. We have not examined this, but it is likely that, at most, a single cross section per nuclide will be adequate and even fewer two-nuclide chains will suffice.

D. Decay Data Testing for ENDF/B-V (T. R. England, W. B. Wilson, and N. L. Whittemore)

Tests of the preliminary spectral data for ENDF/B-V fission product nuclides were completed and supplied to CSEWG. The files currently have decay data for 317 nuclides with 261 having spectral data. (The complete fission-product file will contain 877 nuclides, but only the 261 will have detailed spectral data --

this is an increase of 81 nuclides having spectra over ENDF/B-IV.) The initial testing is for consistency of Q values with decay energies and average beta and gamma energies with the detailed spectra. There are ∿34 nuclides containing some consistency errors of >5%. In addition, comparisons were made with ENDF/B-IV. Sixty nuclides differ by >20% in total recoverable energy or Q value; larger differences in more nuclides are found in average beta and gamma energies. Half-lives agree with ENDF/B-IV within 10%, except for 40 nuclides.

All differences are being investigated at the Idaho National Engineering Laboratory, Hanford Engineering Development Laboratory, and Los Alamos Scientific Laboratory.

E. ANS 5.1 Decay Power Standard (T. R. England, R. J. LaBauve, W. B. Wilson, and N. L. Whittemore)

The ANS 5.1 decay power standard committee met in Atlanta on June 4, 1979. The new standard has now completed all review processes and should be published for general distribution as an ANSI Standard by August or September.

There are known deficiencies in the standard. In particular, the treatment of absorption effects requires a more precise methodology in the absence of detailed summation calculations. A method developed at LASL (T-2) was presented and accepted as a workable technique for future versions of the standard (See Sec. III-B). In addition, the T-2 calculation of actinide heating show that more nuclides must be included than simply the ^{239}U and ^{239}Np actinides now in the standard.

Figures 10 and 11 show fractions of each actinide contribution vs. decay time for a ^{235}U-^{238}U fueled LWR system and a ^{232}Th-^{233}U system, each irradiated for 34 000 MWd/t. Figures 12 and 13 show the total fission product and actinide contributions for each system. Figure 14 compares a conceptual upper-bound actinide correction to the ANS 5.1 fission-product decay-heat standard with the upper bound correction for absorption effects, G_{max}, contained in the standard. The actinide correction is limited to ^{235}U-^{238}U fuel case studies, which varied from 0.1 to 34 Gwd/t.

Finally, measurements of ^{233}U heating at LASL and ^{241}Pu at ORNL will probably be used, along with summation calculations, in a future extension of the standard.

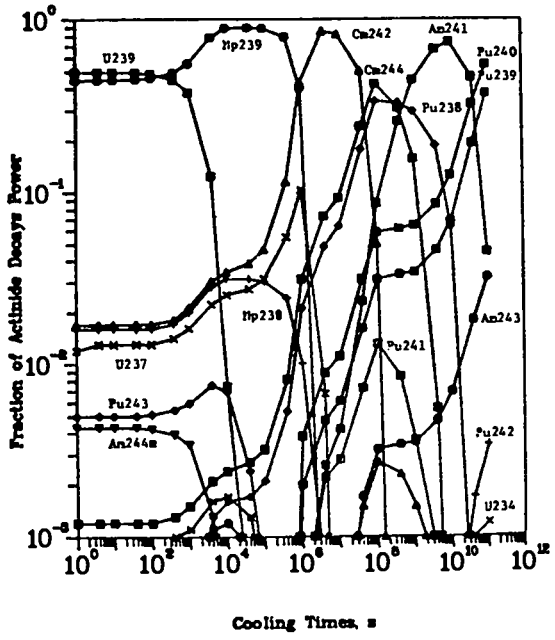

Fig. 10.
Nuclide contributors to actinide decay power, PWR 2.561% $^{235}U/^{238}U$ fuel, 34 GWD/MT, 1082 days.

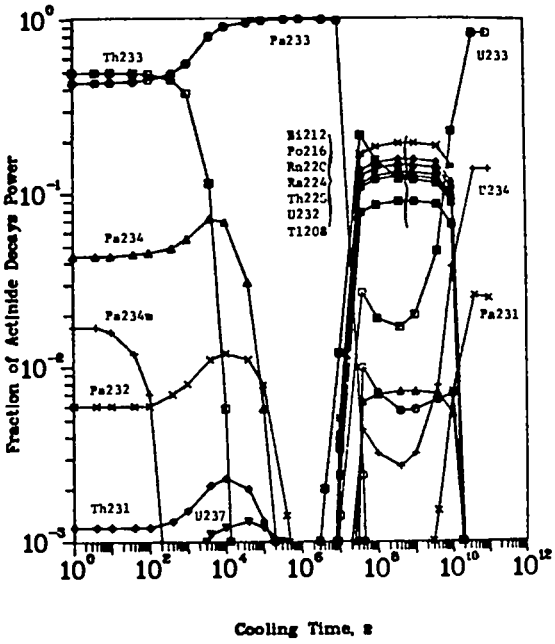

Fig. 11.
Nuclide contributors to actinide decay power, PWR 2.95% $^{233}U/^{232}Th$ fuel, 34 GWD/MT, 835 days.

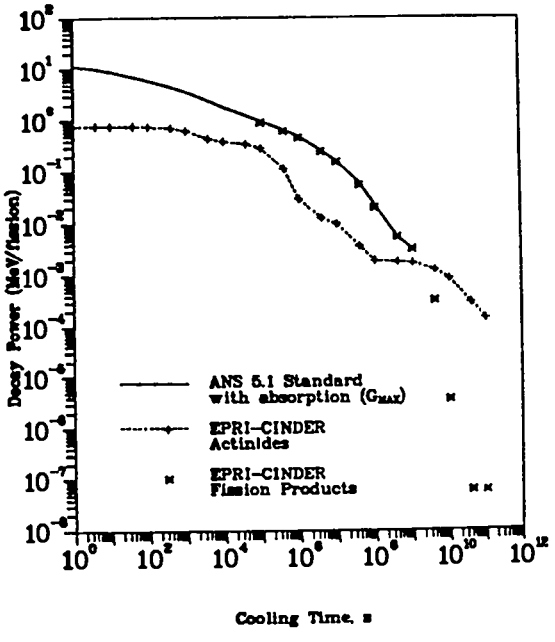

Fig. 12.
Fission product and actinide decay power, PWR 2.561% $^{235}U/^{238}U$ fuel, 34 GWD/MT, 1082 days.

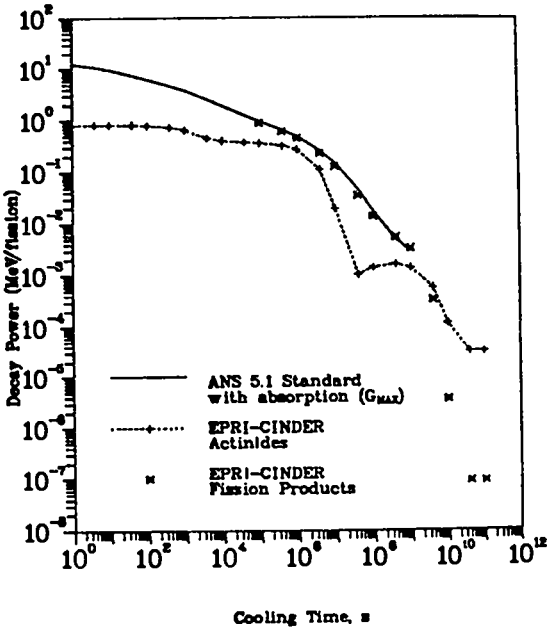

Fig. 13.
Fission product and actinide decay power, PWR 2.95% $^{233}U/^{232}Th$ fuel, 34 GWD/MT, 835 days.

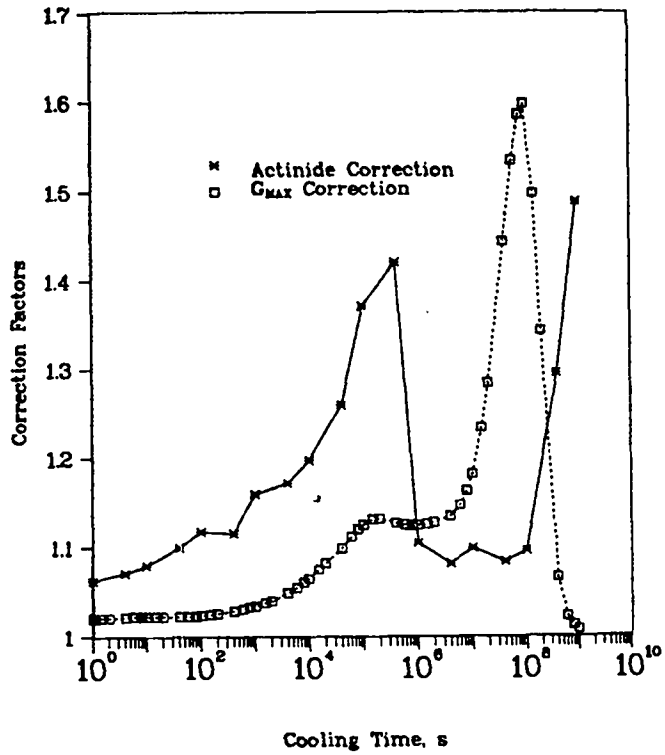

Fig. 14.
Conceptual upper-bound actinide decay power correction factor for $^{235}U/^{238}U$-fueled LWRs.

F. Three Mile Island Calculations (W. B. Wilson, T. R. England, R. J. LaBauve, and N. L. Whittemore)

Calculations of decay heating source terms (fission products and actinides), beta- and gamma-decay spectra, and gas content following the TMI-2 incident were requested by Electric Power Research Institute, Nuclear Regulatory Commission, (NRC), and more recently, by the President's TMI Commission. A large amount of data was supplied based on an assumed full power operation for 88 days prior to the incident on March 28, 1979. More recently, we generated a variable power history from the Metropolitan Edison monthly operating reports to NRC. All calculations were repeated using the new history provided in Table XII and Fig. 15. The heating (alpha, beta, and gamma) from actinides and fission products using the history is given in Table XIII and Fig. 16. Figure 17 shows the component heating from actinides and fission products.

Heating values apply for the total core, assuming all products are present. Some fraction of the heating is due to the escaping gases and volatile products; therefore, these results represent an upper limit of the total core value. Work on this project is continuing.

TABLE XII

CINDER HISTOGRAM CORE POWER HISTORY
THREE MILE ISLAND, UNIT 2

Period	Start Time/date	End Time/date	Δt (h)	Elapsed Time (h)	Ave. Power Mw(th)
1	0300/4-21-78	1700/4-23-78	62.0	62.0	611.6
2	1700/4-23-78	2030/9-17-78	3531.5	3593.5	0.0
3	2030/9-17-78	2400/9-30-78	315.5	3909.0	524.52
4	0000/10-1-78	1400/10-5-78	110.0	4019.0	1109.0
5	1400/10-5-78	2400/10-12-78	178.0	4197.0	0.0
6	0000/10-13-78	0500/10-28-78	365.0	4562.0	1488.94
7	0500/10-28-78	1400/11-1-78	105.0	4667.0	0.0
8	1400/11-1-78	2400/11-3-78	58.0	4725.0	2397.8
9	0000/11-4-78	0230/11-5-78	26.5	4751.5	0.0
10	0230/11-5-78	0530/11-7-78	51.0	4802.5	2034.1
11	0530/11-7-78	1800/12-3-78	636.5	5439.0	0.0
12	1800/12-3-78	0200/12-16-78	296.0	5735.0	2104.09
13	0200/12-16-78	0700/12-22-78	149.0	5884.0	0.0
14	0700/12-22-78	2400/12-31-78	233.0	6117.0	2467.3
15	0000/1-1-79	0800/1-14-79	320.0	6437.0	2281.8
16	0800/1-14-79	1440/1-31-79	414.67	6851.67	0.0
17	1440/1-31-79	2400/1-31-79	9.33	6861.0	33.4
18	0000/2-1-79	2400/2-28-79	672.0	7533.0	2462.14
19	0000/3-1-79	1545/3-6-79	135.75	7668.75	2743.5
20	1545/3-6-79	0815/3-7-79	16.5	7685.25	0.0
21	0815/3-7-79	2400/3-7-79	15.75	7701.0	1697.6
22	0000/3-8-79	0400/3-28-79	484.0	8185.0	2699.704

TABLE XIII

CORE DECAY POWER -- THREE MILE ISLAND, UNIT 2

Cooling Time [a]	Fission-Product Decay Power, MW [b]			Actinide Decay Power, MW [c]				Total Decay Power, MW			
	Beta	Gamma	Total	Alpha	Beta	Gamma	Total	Alpha	Beta	Gamma	Total
1.00+0 s	8.21+1	7.88+1	1.61+2	3.54-4	5.05+0	1.78+0	6.83+0	3.54-4	8.71+1	8.06+1	1.68+2
4.00+0 s	7.05+1	7.05+1	1.41+2	3.54-4	5.04+0	1.78+0	6.82+0	3.54-4	7.56+1	7.23+1	1.48+2
1.00+1 s	6.05+1	6.29+1	1.23+2	3.54-4	5.04+0	1.78+0	6.81+0	3.54-4	6.55+1	6.47+1	1.30+2
4.00+1 s	4.52+1	5.10+1	9.62+1	3.54-4	4.99+0	1.77+0	6.76+0	3.54-4	5.02+1	5.27+1	1.03+2
1.00+2 s	3.65+1	4.28+1	7.93+1	3.54-4	4.90+0	1.76+0	6.66+0	3.54-4	4.14+1	4.46+1	8.60+1
4.00+2 s	2.65+1	3.24+1	5.90+1	3.54-4	4.48+0	1.70+0	6.19+0	3.54-4	3.10+1	3.41+1	6.52+1
1.00+3 s	2.09+1	2.65+1	4.74+1	3.54-4	3.82+0	1.61+0	5.43+0	3.54-4	2.47+1	2.81+1	5.28+1
1.00+0 h	1.40+1	1.78+1	3.17+1	3.55-4	2.41+0	1.42+0	3.83+0	3.55-4	1.64+1	1.92+1	3.56+1
2.00+0 h	1.10+1	1.40+1	2.51+1	3.55-4	1.94+0	1.35+0	3.29+0	3.55-4	1.30+1	1.54+1	2.84+1
5.00+0 h	8.26+0	1.01+1	1.84+1	3.55-4	1.78+0	1.29+0	3.07+0	3.55-4	1.00+1	1.14+1	2.14+1
1.00+1 h	6.37+0	8.11+0	1.45+1	3.56-4	1.68+0	1.21+0	2.89+0	3.56-4	8.05+0	9.32+0	1.74+1
2.00+1 h	4.87+0	6.45+0	1.13+1	3.58-4	1.48+0	1.07+0	2.56+0	3.58-4	6.35+0	7.52+0	1.39+1
5.00+1 h	2.73+0	4.43+0	7.15+0	3.61-4	1.03+0	7.43-1	1.77+0	3.61-4	3.76+0	5.17+0	8.93+0
1.00+2 h	2.13+0	3.50+0	5.63+0	3.64-4	5.60-1	4.04-1	9.65-1	3.64-4	2.69+0	3.90+0	6.59+0
2.00+2 h	1.65+0	2.61+0	4.26+0	3.66-4	1.67-1	1.21-1	2.88-1	3.66-4	1.82+0	2.73+0	4.55+0
5.00+2 h	1.08+0	1.50+0	2.58+0	3.66-4	5.46-3	4.11-3	9.94-3	3.66-4	1.09+0	1.50+0	2.59+0
1.00+3 h	7.07-1	8.54-1	1.56+0	3.64-4	1.75-4	1.45-4	6.84-4	3.64-4	7.08-1	8.54-1	1.56+0
2.00+3 h	4.28-1	4.55-1	8.83-1	3.61-4	6.92-6	2.01-6	3.69-4	3.61-4	4.28-1	4.55-1	8.83-1
5.00+3 h	1.89-1	1.34-1	3.22-1	3.55-4	4.60-6	1.03-7	3.60-4	3.55-4	1.89-1	1.34-1	3.23-1
1.00+0 y	1.06-1	3.33-2	1.40-1	3.52-4	4.52-6	1.17-7	3.57-4	3.52-4	1.06-1	3.33-2	1.40-1
1.00+4 h	9.22-2	2.27-2	1.15-1	3.52-4	4.49-6	1.21-7	3.57-4	3.52-4	9.22-2	2.27-2	1.15-1
2.00+4 h	3.73-2	5.85-3	4.32-2	3.56-4	4.29-6	1.60-7	3.60-4	3.56-4	3.73-2	5.85-3	4.35-2
5.00+4 h	7.66-3	3.23-3	1.09-2	3.75-4	3.76-6	2.66-7	3.80-4	3.75-4	7.66-3	3.23-3	1.13-2

[a] Read as 1.00×10^{0} seconds.

[b] Fission-product total decay power values were calculated with the DKPOWR code for cooling times $tc \leq 20$ h, using the fission pulse functions and upper-bound absorption correction Gmax of the recent ANS Standard 5.1, "Decay Heat Power in Light Water Reactors." The beta and gamma components of fission-product decay power were obtained using beta and gamma decay power fractions calculated with CINDER-10 (for $tc \leq 20$ h) and EPRI-CINDER (for $tc > 20$ h). All fission-product decay power quantities for $tc > 20$ h were calculated with EPRI-CINDER.

[c] Actinide alpha, beta, gamma, and total decay power values are from tandem EPRI-CELL/EPRI-CINDER calculations.

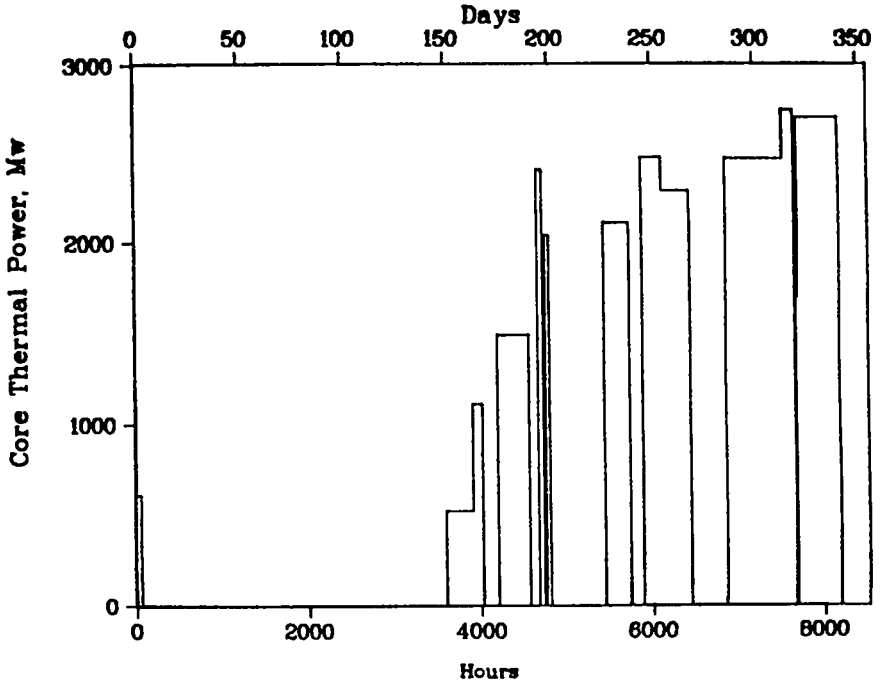

Fig. 15.
CINDER histogram core power history, Three Mile Island Unit 2.

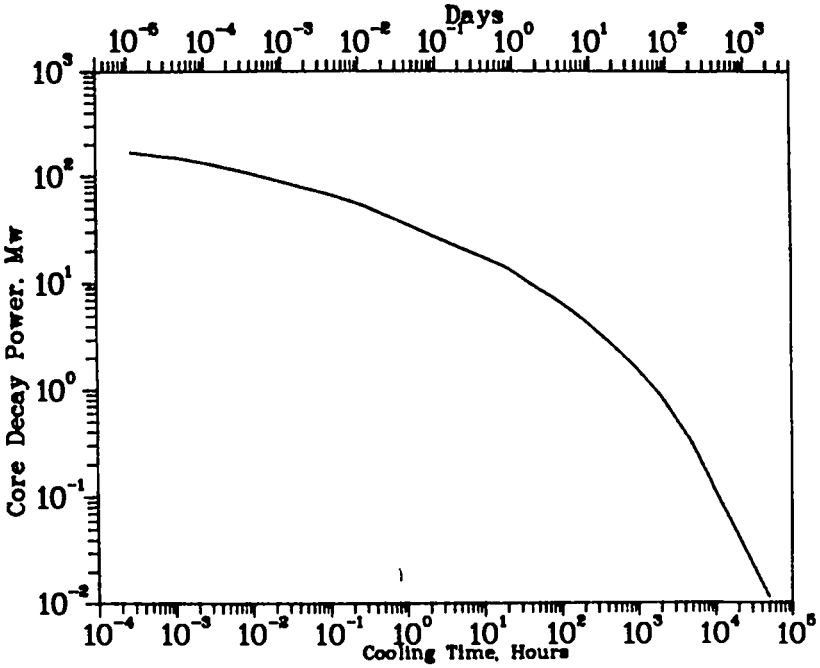

Fig. 16.
Total core decay power from actinides and fission products. Three Mile Island, Unit 2.

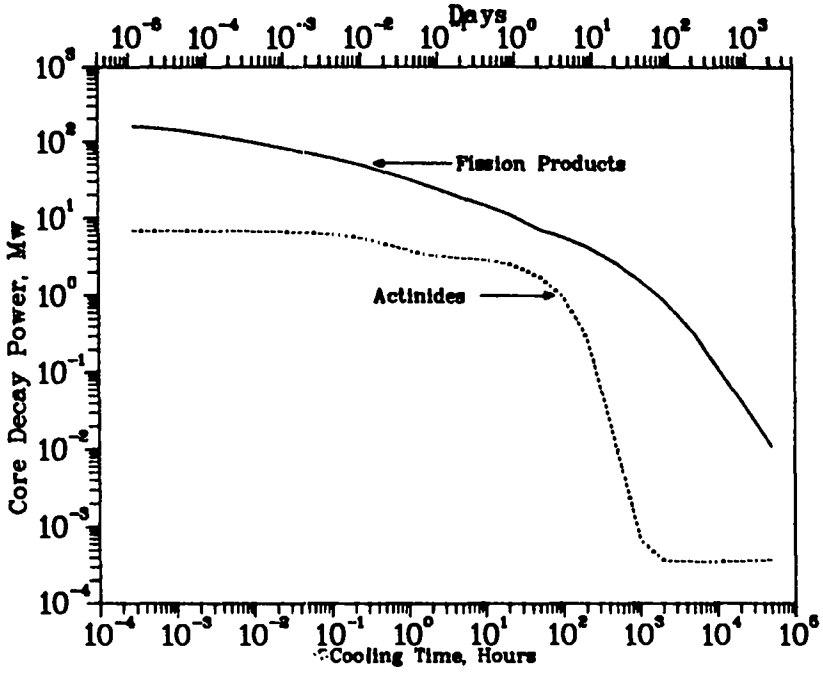

Fig. 17.
Actinide and fission-product decay power components. Three Mile Island Unit 2.

G. Decay Spectral Comparisons (T. R. Englnad, N. L. Whittemore, and D. George)

Oak Ridge National Laboratory (ORNL) (J. K. Dickens) has supplied detailed time-dependent gamma and beta decay spectra for ^{239}Pu following thermal fission for 1, 5, and 100 s periods. We have run CINDER-10 calculations for each case and reinstated codes necessary for comparisons between calculation and experiment. These comparisons will be supplied to ORNL for use in a joint report. More than 40 spectra of each type are being compared, each involving 150 or more energy points. Calculations are complete, but comparison plots have not been made.

H. CINDER-10 Code [T. R. England; N. L. Whittemore; and R. Wilczynski (Bettis Atomic Power Laboratory)]

Work has resumed on modifications of CINDER-10 to reduce storage requirements and running times. Except for data libraries and selected routines, the work is being done jointly with Bettis Atomic Power Laboratory.

REFERENCES

1. G. M. Hale and D. C. Dodder, "R-Matrix Analysis of the ^{7}Li System," in "Applied Nuclear Data Research and Development, January 1-March 31, 1977," Los Alamos Scientific Laboratory report LA-6893-PR, p. 1 (1977).

2. D. C. Dodder, G. M. Hale, S. D. Baker, and E. K. Biegert, "Charge Symmetric R-Matrix Analysis of the Seven-Nucleon System," in "Applied Nuclear Data Research and Development, July 1-September 30, 1978," Los Alamos Scientific Laboratory report LA-7596-PR, p. 1, (1978).

3. G. M. Hale, "Fusion Reactions," in "Applied Nuclear Data Research and Development, October 1-December 31, 1978," Los Alamos Scientific Laboratory report LA-7722-PR, p. 1 (1978).

4. G. M. Hale and D. Dodder, "Reaction Rates for $^{6}Li(p,\alpha)^{3}He$," in Brookhaven National Laboratory report BNL-NCS-26133, p. 128 (1979).

5. D. C. Dodder and G. M. Hale, "Applications of Approximate Isospin Conservation in R-Matrix Analyses," Proc. of Intnl. Conf. on Neutron Physics and Nuclear Data, Harwell, p. 490 (1978).

6. A. J. Elwyn, Argonne National Laboratory, personal communication (1979).

7. G. M. Hale, "R-Matrix Analysis of the ^{7}Li System," Proc. Intn'l. Specialists Symposium on Neutron Standards and Applications (NBS Special Publications 493), p. 30 (1977).

8. S. D. Baker, E. K. Biegert, D. C. Dodder, and G. M. Hale, "Low Energy $^{6}Li(p,^{3}He)^{4}He$ Cross Section," submitted to Astrophys. J. (1979).

9. P. G. Young and L. Stewart, "Evaluated Data for n + ^{9}Be Reactions," Los Alamos Scientific Laboratory report LA-7932-MS (ENDF-283), (1979).

10. D. M. Drake, G. F. Auchampaugh, E. D. Arthur, C. E. Ragan, and P. G. Young, "Double-Differential Beryllium Neutron Cross Sections at Incident Neutron Energies of 5.9, 10.1, and 14.2 MeV," Nucl. Sci. Eng. 63, 401 (1977).

11. H. H. Hogue, P. L. Von Behren, D. H. Epperson, S. G. Glendinning, P. W. Lisowski, C. E. Nelson, H. W. Newson, F. O. Purser, W. Tornow, C. R. Gould, and L. W. Seagondollar, "Differential Elastic and Inelastic Scattering of 7- to 15-MeV Neutrons from Beryllium," Nucl. Sci. Eng. 68, 38 (1978).

12. E. D. Arthur, "Calculation of Neutron Cross Sections on Isotopes of Yttrium and Zirconium," Los Alamos Scientific Laboratory report LA-7789-MS (1979).

13. C. H. Johnson, A. Galonsky, and C. N. Inskeep, "Cross Sections for (p,n) Reactions in Intermediate-Weight Nuclei," Oak Ridge National Laboratory report ORNL-2910 (1960) (Unpublished).

14. Leona Stewart, "Hydrogen Scattering Cross Section, $^{1}H(n,n)^{1}H$," Los Alamos Alamos Scientific Laboratory report LA-7899-MS (1979).

15. Computer tapes and additional information on ENDF/B-V can be obtained from the National Nuclear Data Center at Brookhaven National Laboratory, Upton, New York 11973.

16. E. M. Bohn, R. Maerker, B. A. Magurno, F. J. McCrosson, and R. E. Schenter, Eds., "Benchmark Testing of ENDF/B-IV, Vol. I," Brookhaven National Laboratory report BNL-NC5-21118 (ENDF-230) (March 1976), Chap. IV.

17. C. I. Baxman and P. G. Young, "Applied Nuclear Data Research and Development April 1--June 30, 1977," Los Alamos Scientific Laboratory report LA-6971-PR (1977), p. 21.

18. C. I. Baxman and P. G. Young, "Applied Nuclear Data Research and Development July 1--September 30, 1978," Los Alamos Scientific Laboratory Report LA-7596-PR (1978), p. 16.

19. M. A. Abdou, C. W. Maynard, and R. Q. Wright, "MACK: A Computer Program to Calculate Neutron Energy Release Parameters (Fluence-to-KERMA Factors) and Multigroup Neutron Reaction Cross Sections from Nuclear Data in ENDF Format," Oak Ridge National Laboratory report ORNL-TM-3994 (July 1973).

20. R. E. MacFarlane, R. J. Barrett, D. W. Muir, and R. M. Boicourt, "The NJOY Nuclear Data Processing System: User's Manual," Los Alamos Scientific Laboratory report LA-7584-M (ENDF-272) (December 1978).

21. H. Alter, R. B. Kidman, R. LaBauve, R. Protsik, and B. A. Zolotar, "Cross Section Evaluation Working Group Benchmark Specifications," Brookhaven National Laboratory report BNL-19302 (ENDF-202) (November 1974).

22. R. J. LaBauve, T. R. England, D. C. George, and M. G. Stamatelatos, "The Application of a Library of Processed ENDF/B-IV Fission-Product Aggregate Decay Data in the Calculation of Decay-Energy Spectra," Los Alamos Scientific Laboratory report LA-7483-MS (September 1978).

23. R. J. LaBauve, T. R. England, and W. B. Wilson, "Absorption Effects on Decay Heat and Spectral Pulse Kernels," Trans. Am. Nucl. Soc. 32, 739 (1979).

☆U.S. Government Printing Office: 1979 – 677–013/185

Printed in the United States of America. Available from
National Technical Information Service
US Department of Commerce
5285 Port Royal Road
Springfield, VA 22161

Microfiche $3.00

001-025	4.00	126-150	7.25	251-275	10.75	376-400	13.00	501-525	15.25
026-050	4.50	151-175	8.00	276-300	11.00	401-425	13.25	526-550	15.50
051-075	5.25	176-200	9.00	301-325	11.75	426-450	14.00	551-575	16.25
076-100	6.00	201-225	9.25	326-350	12.00	451-475	14.50	576-600	16.50
101-125	6.50	226-250	9.50	351-375	12.50	476-500	15.00	601-up	

Note: Add $2.50 for each additional 100-page increment from 601 pages up.